

1 **The impact of multi-decadal changes in VOCs speciation on urban** 2 **ozone chemistry: A case study in Birmingham, United Kingdom.**

3 Jianghao Li^{1,2}, Alastair C. Lewis^{1,3}, Jim R. Hopkins^{1,3}, Stephen J. Andrews^{1,3}, Tim Murrells⁴, Neil
4 Passant⁴, Ben Richmond⁴, Siqi Hou⁵, William J. Bloss⁵, Roy M. Harrison^{5,6}, Zongbo Shi⁵.

5 ¹Wolfson Atmospheric Chemistry Laboratories, University of York, York YO10 5DD, UK

6 ²School of Water and Environment, Chang'an University, Xi'an 710064, China

7 ³National Centre for Atmospheric Science, University of York, Heslington, York YO10 5DD, UK

8 ⁴Ricardo Energy and Environment Gemini Building, Fermi Avenue, Harwell, Oxon OX11 0QR, UK

9 ⁵School of Geography, Earth and Environmental Sciences, University of Birmingham, Edgbaston,
10 Birmingham B15 2TT, UK

11 ⁶Department of Environmental Sciences, Faculty of Meteorology, Environment and Arid Land
12 Agriculture, King Abdulaziz University, P.O. Box 80208, Jeddah 21589, Saudi Arabia

13 *Correspondence to:* Jianghao Li (cfm531@york.ac.uk)

14
15 **Abstract** Anthropogenic non-methane volatile organic compounds (VOCs) in the United Kingdom
16 have been substantially reduced since 1990, in part attributed to controls on evaporative and vehicle
17 tailpipe emissions. Over time other sources with a different speciation, for example alcohols from
18 solvent use and industry processes, have grown in both relative importance and in some cases in
19 absolute terms. The impact of this change in speciation and the resulting photochemical reactivities
20 of VOCs are evaluated using a photochemical box model constrained by observational data during
21 a summertime ozone event (Birmingham, UK), and apportionment of sources based on the UK
22 National Atmospheric Emission Inventory (NAEI) data over the period 1990-2019. Despite road
23 transport sources representing only 3.3% of UK VOC emissions in 2019, it continued as the sector
24 with the largest influence on local O₃ production rate (P(O₃)). Under case study conditions, the 96%
25 reduction in road transport VOC emissions that has been achieved between 1990 – 2019 has likely
26 reduced daytime P(O₃) by ~1.67 ppbv h⁻¹. Further abatement of fuel fugitive emissions was modeled
27 to have had less impact on P(O₃) reduction than abatement of VOCs from industrial processes and
28 solvent use. The long-term trend of increased emissions of ethanol and methanol have somewhat
29 weakened the benefits of reducing road transport emissions, increasing P(O₃) by ~0.19 ppbv h⁻¹ in

30 the case study. Abatement of VOC emissions from multiple sources has been a notable technical
31 and policy success in the UK but some future benefits (from an ozone perspective) of the phase out
32 of internal combustion engine passenger cars may be offset if domestic and commercial solvent use
33 of VOCs were to continue to increase.

34

35 **1. Introduction**

36 Elevated tropospheric ozone (O_3) has been a long-standing pollutant of concern in the rural
37 and sub-urban environment and is now becoming more prevalent in urban centers as primary NO
38 traffic emissions reduce (Sicard, 2021). As an important tropospheric oxidant and greenhouse gas
39 (Kumar et al., 2021), exposure to O_3 also increases risks of mortality from respiratory diseases and
40 adversely impacts on crop productivity (Lefohn et al., 2018). O_3 is mainly formed through
41 photochemical reactions involving the oxidation of volatile organic compounds (VOCs) in the
42 presence of nitrogen oxides (NO_x , $NO_x=NO+NO_2$) (Calvert et al., 2015). The release of VOCs arises
43 from a wide range of activities, including unburned fuel or partially combusted products in exhaust,
44 from solvents used in industry and numerous other diffuse domestic and commercial sources (He et
45 al., 2019). Effective policies to mitigate ozone pollution rely on an accurate estimate of both
46 emissions and speciation of O_3 precursors.

47 The challenge in reducing O_3 lies in its non-linear relationship with its precursors since
48 individual VOCs have unique capacities for forming ozone. Decades of modelling studies have
49 established regimes where reductions in NO_x or VOCs emissions would be preferentially beneficial
50 to mitigate O_3 – so-called NO_x -limited or VOC-limited regimes (Seinfeld and Pandis, 2016).
51 Abatement of VOCs sources is important in VOCs-limited areas since decreasing the emissions can
52 effectively reduce the local O_3 production rate and help limit O_3 peak concentrations (Gaudel et al.,
53 2020). The wide range of sources, including many that are diffuse and occur indoors, and differing
54 photochemical reactivities further complicates O_3 reduction strategies. Different mixes of sources
55 and speciation can lead to a need for localized policies. For example, short-chain alkanes and
56 alkenes with high hydroxyl radical reactivity emitted from on-road transportation in China, have
57 been reported as being responsible for 26% of national O_3 formation (Wu and Xie, 2017). A field
58 observation study in Delhi, India reported that the O_3 production in that city was most sensitive to

59 monoaromatics, followed by monoterpenes and alkenes during a post-monsoon period in 2018
60 (Nelson et al., 2021). Another study at urban sites in Seoul, South Korea concluded that the O₃
61 production was controlled by C>6 aromatics and isoprene during a summer O₃ episode in 2016
62 (Schroeder et al., 2020). There is therefore no ‘one size fits-all’ policy in terms for which sources
63 and sectors to target for optimal O₃ abatement efforts.

64 Policy and regulation aimed at improving air quality in many countries including the United
65 States, the United Kingdom and Europe have led to decades of falling VOCs emissions (Lewis et
66 al., 2020; Coggon et al., 2021). This reduction can be substantially attributed to the successful
67 technical implementation of tailpipe exhaust after-treatment technology for gasoline vehicles
68 controls on evaporative emissions from vehicles including during re-fueling and a more widespread
69 set of efforts to control industrial emissions (Winkler et al., 2018). Despite these successes, O₃
70 remains a pollutant of concern; whilst peak concentrations during O₃ events have reduced in the UK,
71 increases in the long-term urban background O₃ concentrations have been observed since the 1990s
72 (Department for Environment, Food & Rural Affairs, 2023). A variety of explanations have been
73 given to account for the increase including a rising northern hemisphere background O₃, increasing
74 methane which contributes to both global radiative forcing and enhances O₃ production (Tarasick et
75 al., 2019; Abernethy et al., 2021), the increases in non-vehicular sources of VOCs emissions
76 (McDonald et al., 2018; Yeoman and Lewis, 2021), and the reduction of NO_x in VOCs-limited urban
77 areas leading to greater O₃ production efficiency (Sicard et al., 2020).

78 The UK National Atmospheric Emissions Inventory (NAEI) for VOCs has shown increases in
79 the relative contribution of solvent usage and the food & wine industry to total national VOCs
80 emission over 1990-2019, and steady growth in the relative importance of OVOCs within the overall
81 speciation (Lewis et al., 2020). In North America and Europe cities, OVOCs emitted from volatile
82 chemical products (VCP) can outweigh fossil fuel sources for urban VOCs. Modelling results
83 showed that the additional OVOCs from VCP emissions were the most important species for urban
84 O₃ production, increasing the daily maximum O₃ mixing ratio by as much as 10 ppbv in Los Angeles
85 (Qin et al., 2021). Substantial OVOCs emissions can come from unexpected places. For example,
86 alcohols emitted from use of windshield fluid are now estimated to be a larger VOC source from
87 road transport than VOC from the tailpipe in the UK (Cliff et al., 2023). From the perspective of O₃
88 pollution, the benefit of substantial reductions on vehicle emissions, whilst there has been a parallel

89 increasing role for non-industrial solvent usage remains unclear. What effect this shift in speciation
90 is having on ozone chemistry is less well studied. One challenge has been the lack of routine
91 measurement of OVOCs in most national air quality monitoring networks (Air Quality Expert
92 Group, 2020).

93 Recent model analysis of decadal trends of ozone has centred on the association between
94 extreme weather and ozone events and projected changes in ozone concentration under chemical
95 regime change scenarios. Significant decline in the UK experiencing ozone episodes and increase
96 in the background ozone concentration are found over the past three decades (Diaz et al., 2020).
97 Elevated ozone mostly occurs in the late spring and summer during anticyclonic conditions when
98 slow moving air masses from continental Europe contribute to accumulation of precursor emissions
99 and enhance photochemical production of ozone (Hertig et al., 2020; Lewis et al., 2021). Higher
100 temperatures in the late summer increase biogenic VOC emissions and reduce ozone deposition,
101 leading to summertime maximum concentrations (Finch and Palmer, 2020). Several studies pointed
102 out that increasingly hot summer due to climate change may offset gains made in the reduction of
103 ozone event over time (Gouldsbrough et al., 2022; Liu et al., 2022). In term of ozone production
104 sensitivity, reductions in NO emissions have led to decreasing trend in annual average concentration.
105 However, 20% or 40% NO_x emission reductions would lead to increases in average and maximum
106 ozone concentrations in the UK with respect to 2018 (Gouldsbrough et al., 2024). In addition to
107 results on NO_x and VOCs sensitivities, Ivatt et al. (2022) revealed that ozone concentrations in North
108 America and Europe were inhibited by aerosol in the 1970s, and this ‘aerosol-inhibited regime’ has
109 been shifted to Asia by 2014.

110 There have been several recent studies focussed on evaluating the impacts of reductions in
111 anthropogenic sources on ozone production. By integrating the U.S. fuel-based inventory of vehicle
112 emissions (FIVE) into air quality model, McDonald et al. (2018) assessed ozone sensitivity to
113 mobile source NO_x emissions over the Eastern U.S., and Coggon et al. (2021) employed FIVE with
114 volatile chemical products (VCPs) to evaluate contributions of VOC from fossil fuel and different
115 types of VCP emissions to ozone production at an urban background site in New York City. Nelson
116 et al. (2021) used emission inventories from Emission Database for Global Atmospheric Research
117 (EDGAR) to investigate *in-situ* ozone production sensitivity to five inventory source sectors at an
118 urban site in Delhi. Kang et al. (2022) applied two emission inventories in air quality model to

119 evaluate contributions of industry, road transport, power plant, and biogenic emissions to ozone
120 production in Chinese cities. Although great efforts have been made toward identifying crucial VOC
121 sources in regional ozone production, understandings of their roles in urban ozone chemistry in the
122 context of historical changes is still lacking.

123 In this study we evaluate the effects of changing speciation on urban ozone chemistry, using
124 recent field measurements of O₃ and its key precursors such as NO_x, CO, speciated VOCs and
125 OVOCs in Birmingham, UK during August 2022. We combine this with changing speciation and
126 relative amounts of VOCs based on long-trends in the NAEI. The sensitivity of *in-situ* production
127 and OH reactivities of the measured O₃ precursors are investigated by constraining the observational
128 data sets to a zero-dimensional chemical box model. By incorporating the detailed NAEI VOCs
129 emission inventories over the period of 1990-2019 into the model, O₃ formation in Birmingham is
130 used as a case study to quantify the impacts of the real-world changes in VOCs sources on urban O₃
131 production rate. The relative importance of different VOCs functional group classes to O₃
132 production are also evaluated. The results help understand impacts of decades of abating different
133 VOCs-emitting sectors on urban O₃ production, and outline the implications for future O₃ control
134 strategies.

135

136 **2. Materials and Methods**

137 **2.1 Field observations**

138 The observations are taken from the Birmingham NERC Air Quality Supersite during August
139 2022. This is located on the University of Birmingham (52°27'20.2"N 1°55'44.3"W) campus. The
140 site has been in operation for many years, and represents an urban background environment. It is
141 influenced by transport emissions from nearby arterial roads and residential emissions from
142 surrounding area. There are no significant industrial activities within a 4km radius of the site.

143 Continuous measurements of NO, NO₂, CO, CH₄, VOCs, O₃, along with meteorological
144 parameters including air temperature and pressure, relative humidity, wind speed and direction were
145 made. Briefly, NO and NO₂ were measured by a chemiluminescence-based T200 analyzer (Teledyne
146 API., U.S.A.) and the T500U Cavity Attenuated Phase Shift (CAPS) analyzer (Teledyne API.,
147 U.S.A.). The concentration of NO_x was then the statistical sum of NO and NO₂. The mixing ratio of

148 CO were measured by a laser absorption spectroscopy Multi-species Continuous Emissions
149 Monitoring instrument (Enviro Technology Service Ltd., UK) (Li et al., 2020). Manual calibration
150 and span checks for the above instruments were performed every 3 days, and automatic zero
151 calibration was set on daily bases. O₃ was measured by an O₃ analyzer (Model 49i, Thermo Fisher
152 Scientific Inc., U.S.A.) with a minimum detection limit (MDL) of 1.0 ppbv. Meteorological
153 parameters including air temperature and pressure, and relative humidity were obtained from a
154 weather station WS300-UMB weather station (Luff GmbH, Germany). Additionally, Wind speed
155 and direction were measured by a 3-axis ultrasonic anemometer (Gill Instruments Ltd., UK) over
156 the campaign.

157 A gas chromatography-flame ionization detection (GC-FID) analysis system (7890A, Agilent
158 Technologies, U.S.A.) was used to quantify 38 individual VOCs species. Details on instrument
159 settings and quality assurance/quality control methods can be found in (Warburton et al., 2023).
160 Briefly, the GC-FID system utilizes dual detectors: one detector for C₂ – C₆ non-methane
161 hydrocarbons (NMHCs); the other detector for remaining C ≥ 7 hydrocarbons, and polar species
162 such as ethers, ketones, and alcohols. Ambient samples were dried at –40 °C using a water trap and
163 then preconcentrated on a carbon adsorbent at the lowest temperature the unit could achieve, always
164 lower than -115 °C. Once a 0.5L sample had been collected, a pre-concentration trap was warmed
165 slightly from -80 °C to purge trapped atmospheric CO₂. The trap was then heated to 190 °C for 3
166 minutes with a counter flow of helium thermally desorbing the concentrated VOCs onto focusing
167 micro-trap held at lower than -115 °C. The analytes were flash heated and passed onto a VF-WAX
168 column. The unresolved analytes (C₂ – C₆ NMHCs) were then transferred into a Na₂SO₄-deactivated
169 Al₂O₃ porous-layer open tubular (PLOT) column via a Deans switch, for separation and detection
170 by the first FID. The Dean switch then diverted the analytes onto a fused silica internal diameter to
171 balance column flows and subsequently transfer the VF-WAX column- resolved species into the
172 second FID. Generally, quantification of C₂-C₆ hydrocarbons was completed by the first FID using
173 4 ppbv gas standard cylinders (the National Physical Laboratory, Teddington, UK). Quantification
174 of C ≥ 7 hydrocarbons and OVOCs was completed by the second FID using effective carbon number
175 (ECN) with reference to toluene. In this study, the concentration of total VOC (TVOC) was defined
176 as the statistical sum of concentrations of measured individual species, but this is not meant to infer
177 that this represents the total reactive carbon in air, which would always be greater than this value

178 due to unmeasured species. Later in this study we broadly group species according to their chemical
179 function groups, summing into alcohols, ketones, alkanes, alkenes, aromatics, aldehydes, and
180 alkynes.

181 The GC-FID system responses were regularly checked by running direct calibration sequences
182 using the 4 ppbv gas standard cylinders. It was verified there was no FID-response drift over the
183 analyzing period for this study. Additionally, carbon-wise FID responses for all reported species
184 were calculated to verify the use of ECN as a quantification method. Table S1 lists which species
185 were directly calibrated, and which used equivalent carbon numbers for quantification. Table S2
186 shows effective carbon numbers of species which used carbon-wise responses.

187 2.2 National emission inventory for VOCs

188 Estimates of UK anthropogenic VOC emissions are taken from the NAEI. The NAEI uses a
189 combination of UK-specific methods and default methods as recommended in the European
190 Monitoring and Evaluation Programme (EMEP)/European Environment Agency (EEA) Emission
191 Inventory Guidebook (European Environment Agency, 2016). Further details can be found in (NAEI,
192 2021). The VOC inventory is also disaggregated into inventories for each individual VOC species
193 and details of the speciation process and assumptions can be found in (Passant, 2002) and (Lewis et
194 al., 2020).

195 Methods to estimate emissions can be divided into two groups: those using emission factors,
196 and those using 'point source' emissions data reported to regulators by the operators of individual
197 industrial sites. The emission factor methods require UK activity data, for example consumption of
198 paint, consumption of a fuel, production of steel or vehicle kilometers travelled. The activity data is
199 then combined with an emission factor which expresses the total VOC emission that is expected per
200 unit of a given activity. Most total VOC emission factors are taken from the internationally applied
201 EMEP/EEA Emission Inventory Guidebook and so are not necessarily UK-specific. The factors for
202 road transport are directly calculated for the UK and a particularly detailed approach is used to
203 estimate emissions using emission factors from the Guidebook for many different vehicle types and
204 emission standards, fuels and road types combined with detailed transport activity from the UK
205 Department for Transport. Government statistics cannot always provide the necessary activity data
206 for other sectors, so industry data are used instead. For instance, NAEI data on consumption of
207 products containing organic solvents are from industry sources. The alternative point source method

208 can be used for source categories where emissions data can be obtained for all sites within the sector,
209 and this limits the method to source categories such as crude oil refining, steel production and
210 chemicals production. The emissions data reported by the operators of these sites can be based on
211 emissions monitoring, although this is not always the case and emissions might instead be estimated,
212 for example, using emission factors.

213 The NAEI produces updates to the inventory for total VOC mass emissions by source sector
214 each year to achieve a consistent historic time-series reflecting trends in UK emissions. Emissions
215 of individual VOC species are estimated using source-specific speciation profiles which show the
216 mass fraction of each species, or in some cases groups of species, emitted by the source (NAEI,
217 2021; Passant, 2002). Over 600 individual VOC species or species groups are included in the
218 speciation, based on sources in industry, regulators and in some cases literature sources and
219 databases such as the USEPA SPECIATE database. The speciated inventory tends to be more
220 uncertain than the estimation of total mass of VOC emissions. The inventory for total VOC mass is
221 updated annually, whereas the speciation profiles are only periodically updated when new
222 information becomes available. Thus, trends in a particular species for a sector are a reflection of
223 changes in total VOC emissions for the sector and do not normally reflect any changes over time in
224 the speciation profile of the sector which may have occurred.

225 2.3 Photochemical box model

226 The framework for evaluating effects of changing VOCs speciation is a 0-D Atmospheric
227 Modelling chemistry box model (Wolfe et al., 2016), driven by the Version 3.3.1 of the Master
228 Chemical Mechanism (MCM v3.3.1) (Saunders et al., 2003; Jenkin et al., 2003). The model can be
229 effective in identifying the instantaneous *in-situ* O₃ sensitivity to changes in individual VOCs. The
230 measured concentrations of 38 VOCs species, NO_x, and CO, along with air temperature and pressure,
231 and relative humidity were averaged to a time resolution of 1-hour to constrain the model. A 3-day
232 model spin-up, with each 24-hour model run constrained by the observational data, was performed
233 in order to initialize the unmeasured compounds and transient radicals. The modelled outputs on the
234 4th day were taken as representing steady state of the photochemistry.

235 Photolysis rates were calculated as a function of solar zenith angle (Saunders et al., 2003):

$$236 \quad J = l(\cos \chi)^m \exp(-n \sec \chi) \quad (1)$$

237 Where J is the photolysis rate in s⁻¹; l , m , n are constants derived from radiative transfer model

238 runs for clear sky condition at an altitude of 0.5 km and literature cross sections/quantum yields; χ
 239 is the solar zenith angle in radians.

240 The net production rate of O₃ ($P(O_3)$) is calculated by the difference of the production rate of
 241 O₃ and the destruction rate of O₃, as in Equation (2):

$$\begin{aligned}
 P(O_3) = & (k_{HO_2+NO}[HO_2][NO] + \sum_i k_{RO_2_i+NO}[RO_2][NO]) - \\
 & (k_{O^1D+H_2O}[O^1D][H_2O] + k_{O_3+OH}[O_3][OH] + k_{O_3+HO_2}[O_3][HO_2] \\
 & k_{NO_2+OH}[NO_2][OH] + \sum_i k_{RO_2_i+NO_2}[RO_2][NO_2])
 \end{aligned} \quad (2)$$

243 Where the former part is the rate of O₃ production, representing by rate of NO oxidation by
 244 HO₂ and RO₂ radicals; the latter part is the destruction rate of O₃, calculating by the sum of the rate
 245 of O₃ photolysis, the rates of the reactions with OH and HO₂ radicals, and the rates of NO₂ loss
 246 through reactions with OH and RO₂ radicals.

247 The sensitivity of O₃ to its precursors is quantified by the index of relative incremental
 248 reactivity (RIR) (Liu et al., 2022b), as in Equation (3):

$$RIR = \frac{\Delta P(O_3)}{P(O_3)} \times a^{-1} \quad (3)$$

249 Where RIR is the Relative Incremental Reactivity in %/%, $\Delta P(O_3)/P(O_3)$ is the ratio of the
 250 change in O₃ production rate to the base O₃ production rate; a is the reduction percentage in the
 251 input concentration of O₃ precursors – a factor that allows for the effects of changing absolute
 252 amounts of VOCs to be evaluated. Here a value of 30% was adopted for a .

254

255 3. Results and Discussion

256 3.1 Observation overview

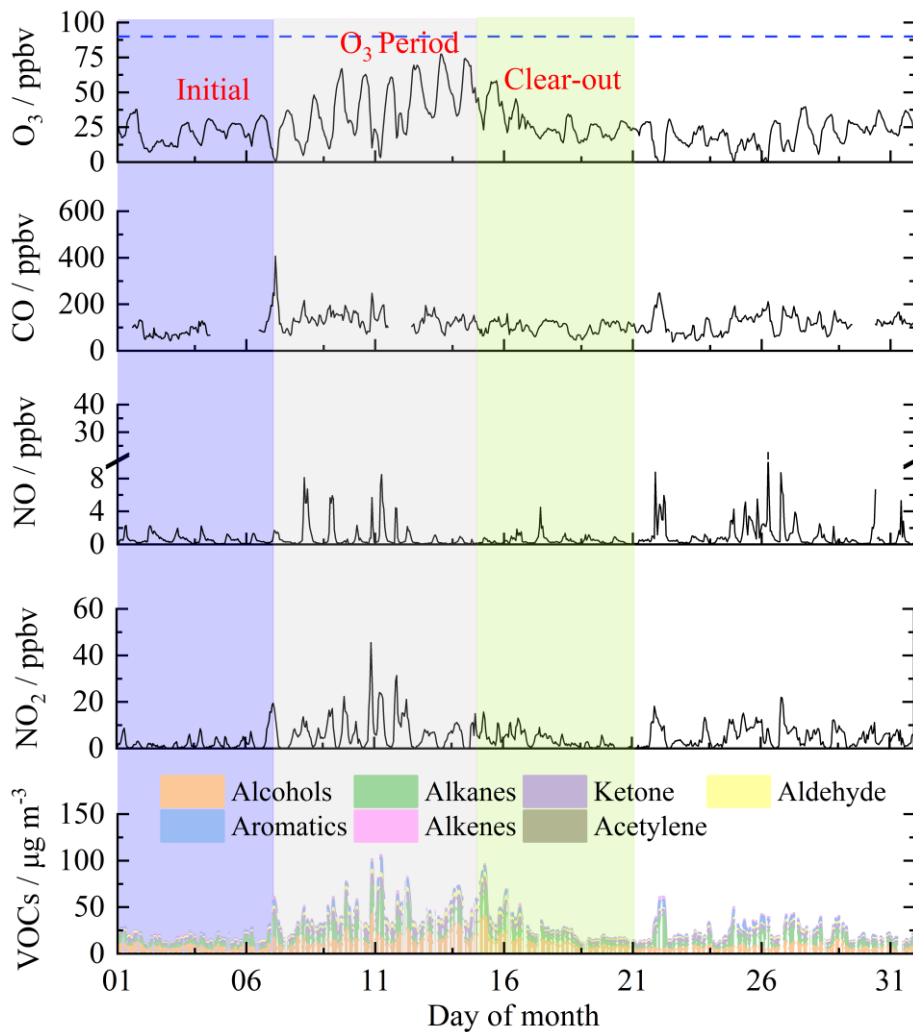
257 The time series of O₃ and its precursors during August 2022 are shown in Figure 1, subdivided
 258 into periods that will be referred to as ‘initial period’, ‘O₃ period’, and ‘clear-out’. The three periods
 259 covered 1st August-21th August 2022. Each period included one full week to avoid
 260 weekday/weekend differences in NO_x and VOCs concentrations impacting differently when O₃
 261 production was compared between the three periods (de Foy et al., 2020). Ozone showed a generally
 262 increasing trend from 1st to 14th August and then returned to relatively low concentrations after 15th
 263 August 2022. The daily maximum 8 h average O₃ concentrations (MDA8h O₃) during the O₃ period
 264 exceeded the WHO guideline value (100 µg m⁻³), ranging from 111 to 153 µg m⁻³. The elevated O₃

265 during the middle of the month corresponded to more intense photochemical formation under hot
266 weather conditions (32.7 °C in maximum) and higher concentrations of O₃ precursors (Table S3).

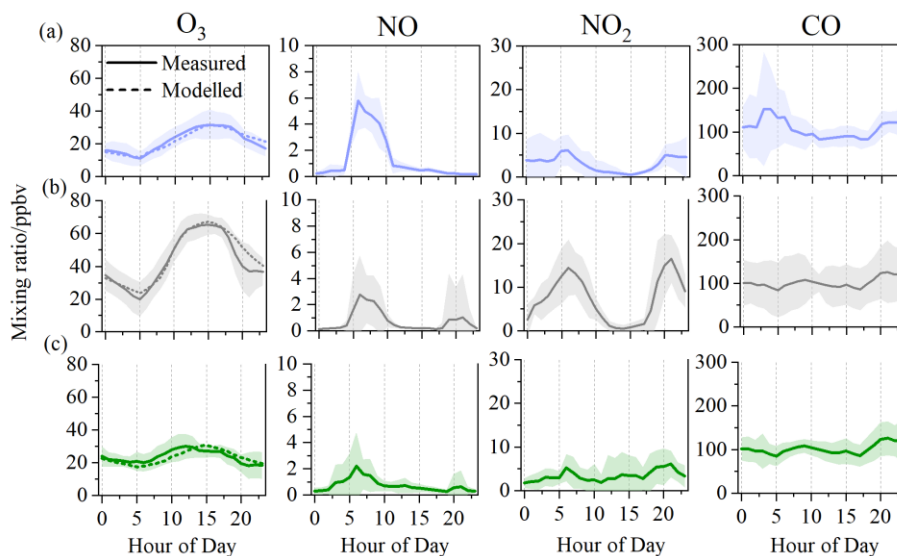
267 The diurnal profile of NO and NO₂ in the three periods generally showed a bimodal pattern,
268 albeit less pronounced in the initial and clear-out periods (Figure 2). The two peaks likely arise as
269 a consequence of increased traffic volumes at the start and end of the day, coupled to boundary layer
270 height changes in the early morning and into the evening (Lee et al., 2020). The average
271 concentrations of NO₂ during 05:00-10:00 were 10.8 ppbv in the O₃ period, which was considerably
272 higher than the concentration of 3.9 ppbv in the initial period and 3.4 ppbv in the clear-out period.
273 The low level of NO in the O₃ period highlights the rapid consumption of NO via photochemical
274 processes. The oxidation of CO is an important source of HO₂ in the atmosphere (Chen et al., 2020),
275 here in the range of 82.5 to 134.2 ppbv with little difference between periods. The diurnal profiles
276 of O₃ peaked at 15:00, with maximum hourly concentrations of 31.6, 67.2, and 30.4 ppbv in the
277 initial, O₃, and clear-out periods, respectively. Slight decreases in O₃ were observed during
278 nighttime (00:00-05:00), indicating enhanced NO titration effects.

279 The detailed VOCs composition in the three periods is presented in Figure S1. Concentration
280 of TVOC were 19.4 ± 8.4 , 48.0 ± 18.8 , and 23.5 ± 12.5 $\mu\text{g m}^{-3}$ in the three periods, respectively.
281 Alcohols, represented mainly by methanol and ethanol, were the predominant group that contributed
282 40.3% - 47.4% of over measured VOCs mass. This was followed by alkanes (21.4%-24.6%) and
283 ketones (16.3%-17.3%). Contributions of aldehyde (acetaldehyde), aromatics, alkenes, and
284 acetylene were low, ranging from 1.0% to 9.4% of total mass. Average mixing ratio of the top 10
285 species in selected periods at Birmingham Supersite are listed in Table S4. The top 10 species were
286 represented by methanol, acetone, ethanol, acetaldehyde, and C₂ – C₄ alkanes across initial period,
287 O₃ period, and clear-out period. The top individual species contributing to the total VOCs were
288 methanol (10.3% – 33.6%) and acetone (15.5% – 17.1%), regardless of the subdivided periods. The
289 results highlight large emissions of ethane, propane, n-butane, and i-butane associated with Natural
290 Gas (NG), Liquefied Petroleum Gas (LPG), and propellant use, fuel combustion and evaporation.
291 Ambient VOCs largely influenced by combustion-related sources (i.e., vehicle exhaust and coal
292 combustion) generally show alkane-dominated composition (Wu and Xie, 2017). Here, the
293 composition and amount of VOCs observed were most likely influenced by non-combustion
294 processes such as volatile chemical product usage and industrial processes (Gkatzelis et al., 2021).

295 Methanol was the most abundant VOC with an average concentration of 4.1 ppbv, followed by
 296 acetone (2.0 ppbv), ethane (1.9 ppbv), ethanol (1.8 ppbv), and acetaldehyde (1.0 ppbv). The average
 297 ratio of ethene/ethane was 0.2 ± 0.1 over the campaign, considerably lower than seen in polluted
 298 locations, e.g. Hong Kong (China) (0.7 ± 0.1) (Wang et al., 2018) and Seremban (Malaysia) (1.1)
 299 (Zulkifli et al., 2022).



300
 301 Figure 1. Time series of O₃, CO, NO, NO₂, and VOCs groups at the Birmingham Supersite. The
 302 blue dash line denotes the national standard (90 ppbv) for hourly O₃ concentration.
 303



304

305 Figure 2. Diurnal variations of O₃, NO, NO₂, and CO during the initial (a), O₃ period (b), and
 306 clear-out period (c). The shaded areas represent standard variations.

307

308 The general diel profiles for all selected VOCs, except for ethane, showed bimodal pattern
 309 (Figure S2). Concentrations were much higher during the night, and lower in the day, due to they
 310 were subject to photochemical losses during the daytime. The bimodal pattern is less apparent for
 311 methanol and acetone, as they are abundant species originating from many anthropogenic sources
 312 in urban areas. For example, methanol was the most abundant species measured at a roadside in UK
 313 using Thermal Desorption-Gas Chromatography coupled with Flame Ionization Detection (TD-GC-
 314 FID) (Cliff et al., 2023). A separate study on gasoline and diesel vehicle exhausts reported methanol
 315 and acetone were the largest OVOCs emitted (Wang et al., 2022). Gkatzelis et al. (2021) conducted
 316 Positive Matrix factorization (PMF) analysis based on observed VOCs dataset in New York City,
 317 and concluded that acetone was the second most abundant species in measurements and was mostly
 318 attributed to volatile consumer product emissions (90%). (See Section 3.3 for further discussions
 319 for anthropogenic sources of OVOCs).

320 3.2 Observation-based O₃ formation sensitivity

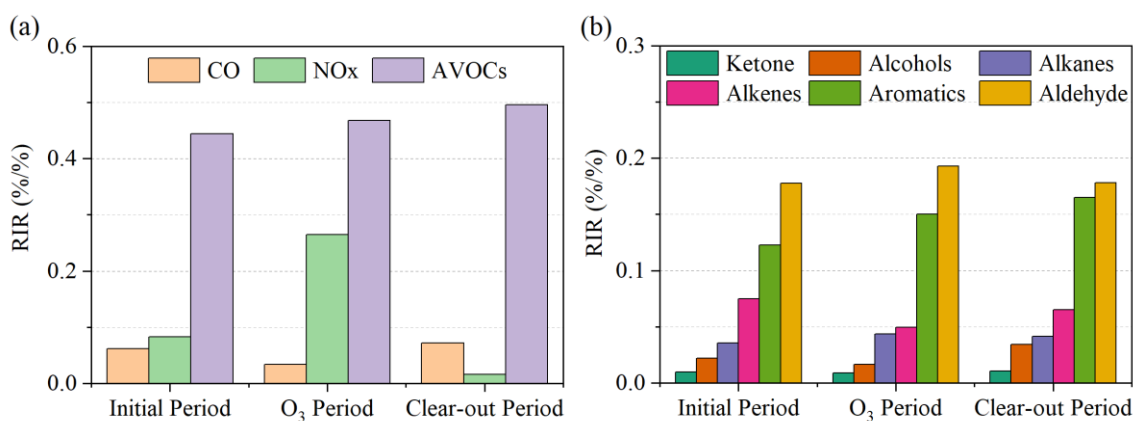
321 The *in-situ* O₃ formation sensitivity was examined via reaction rates of ozone precursors and
 322 OH radical (OH reactivities, ($k(\text{OH})$)) and RIR scales of ozone precursors, along with the chemical
 323 budgets of O₃ formation and loss. In initial and clear-out periods. $k(\text{OH})$ exhibited consistent diurnal
 324 patterns, ranging from 2.4 to 5.9 s⁻¹ (Figure S3). In the O₃ period, $k(\text{OH})$ reached 9.0 and 8.7 s⁻¹ at
 325 approximately 07:00 and 20:00, respectively. A rapid increase in $k(\text{OH})$ was observed in the early

326 morning (00:00-06:00). VOCs and model generated species represented 60.5%, 65.7%, and 56.7%
327 of the total $k(\text{OH})$ in the three periods, respectively. NO_x and CO only contributed 10.2% -27.9% to
328 total $k(\text{OH})$. Among of the VOCs groups, alcohols exhibited the largest $k(\text{OH})$ in all periods,
329 accounting for 5.0% - 6.9% of the total $k(\text{OH})$. The diurnal production and loss of O_3 are shown in
330 Figure S4. The oxidation and photolysis of VOCs promoted the production of RO_2 , and $\text{NO}+\text{RO}_2$
331 contributed 47.7% of the O_3 production pathways in the O_3 period and 36.2% and 39.8% in initial
332 and clear-out periods, respectively. Considering O_3 destruction, $\text{OH}+\text{NO}_2$ was the most important
333 pathway during morning (08:00-12:00), accounting for 73.5%, 55.4% and 59.4% of the O_3
334 destruction pathways in the three periods. The dominant $\text{OH}+\text{NO}_2$ contribution to O_3 destruction
335 suggested that the *in-situ* O_3 productions in all three periods was sensitive to VOCs emissions to
336 some extent.

337 In order to understand contributions of O_3 formation from direct emissions and secondary
338 formations of OVOCs, we developed two modelling scenarios: (1) all OVOCs species were
339 constrained to observed mixing ratio; (2) all OVOCs species were unconstrained. (2) allowed
340 secondary formations of OVOCs by oxidations of their precursor VOCs. As shown in Figure S5,
341 secondary formations of OVOCs had little impact on O_3 formation in all periods. The simulation of
342 O_3 production using the box model without constraining observed OVOCs slightly underestimated
343 average daily maximum O_3 mixing ratio and $\text{P}(\text{O}_3)$, compared to the scenario with all observed
344 OVOCs species constrained. The underestimation for average daily maximum mixing ratio of O_3
345 was 4.8%, 6.9%, and 5.1% in initial period, O_3 period, and clear-out period, respectively. In this
346 case, the underestimation of average daily maximum $\text{P}(\text{O}_3)$ was 5.1%, 6.0%, and 9.3% in the three
347 periods, respectively. The results demonstrated that in the Birmingham case study, primary
348 emissions of OVOCs played central role in the *in-situ* ozone production.

349 The relative incremental reactivity of NO_x , CO, and anthropogenic VOCs (AVOCs, all
350 measured VOCs except for isoprene) are shown in Figure 3. The *in-situ* O_3 production was most
351 sensitive to anthropogenic VOCs with the highest positive RIR values (0.44 - 0.49). This is as
352 anticipated given earlier analyses demonstrating their role in determining $k(\text{OH})$ and O_3 production.
353 The low RIR (0.03 - 0.07) for CO in all three periods indicated a minor contribution of CO oxidation
354 to O_3 production. The high RIR (0.24) for NO_x was only observed in the O_3 period. Acetaldehyde
355 showed the highest positive RIR (0.17 - 0.19) among the AVOCs, suggesting that the photolysis and

356 oxidation of acetaldehyde was a limiting factor for O₃ formation. The important role of carbonyl
 357 compounds in atmospheric photochemistry has also been reported in previous studies, contributing
 358 up to 59.3% to the O₃ formation in ambient environments in China, the United States, and Brazil
 359 (Qin et al., 2021; Liu et al., 2022a; Edwards et al., 2014). Alkanes and alcohols exhibited lower RIR
 360 values (0.02 - 0.04), despite their high mass concentrations.



361

362 Figure 3. Modelled RIRs for (a) major O₃ precursors and (b) the AVOCs groups during
 363 photochemically active daytime (08:00-16:00) in the selected periods. (AVOCs: anthropogenic
 364 VOCs, all measured VOCs except for isoprene)

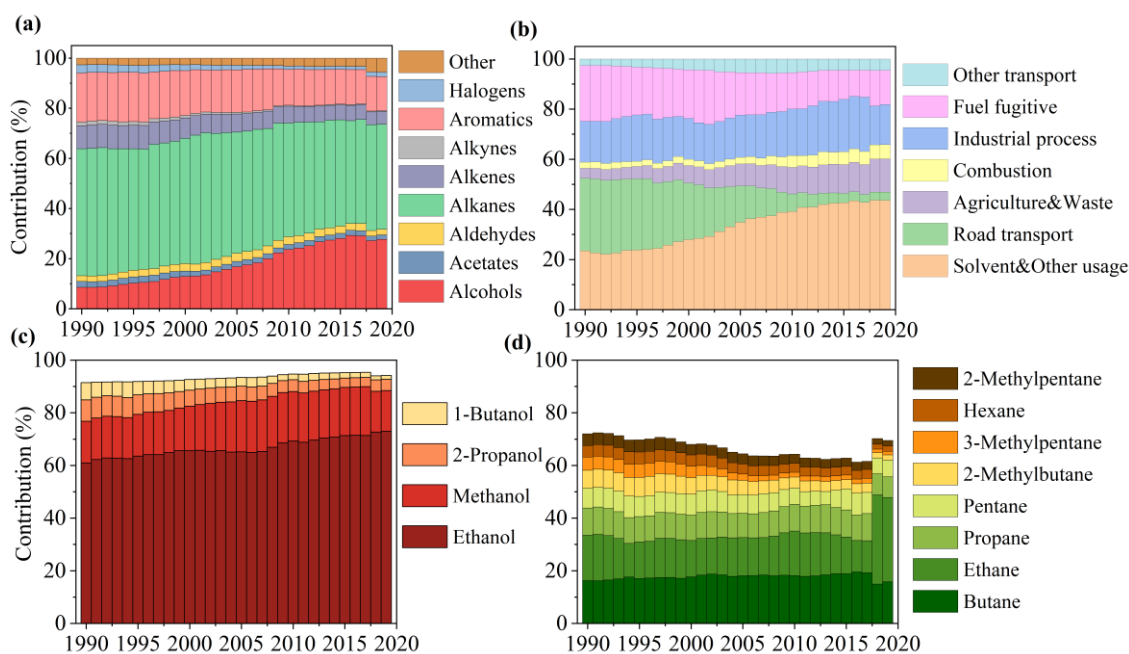
365

366 3.3 Emission inventory-informed O₃ production sensitivity tests

367 The trends in anthropogenic VOCs emissions from 1990 to 2019 estimated by the NAEI are
 368 shown in Figure S6. Over the period, the annual national emissions decreased by ~69.0% from 2,941
 369 kt in 1990 to 911kt in 2019. The reduction is partly attributed to more stringent controls for gasoline
 370 vehicle emissions, both tailpipe and evaporative/fugitive. In 2019, VOCs emissions from on-road
 371 transport and fuel fugitive losses accounted for only 3.3% and 13.7% of the total mass of VOCs
 372 emissions, compared to 29.1% and 26.9% in 1990. Efforts have also been directed towards
 373 controlling industrial processes, commercial solvent usage, and combustion emissions, resulting in
 374 reductions of 66.8%, 48.9%, and 20.7%, respectively over the period. However, contributions from
 375 solvent usage to total VOCs emissions over 1990-2019 showed only modest reductions in the 1990s
 376 and 2000s and indeed small increases in the most recent years (Figure 4(b)). This slight growth in
 377 solvent usage is due to increasing emissions from solvent use in consumer products such as
 378 decorative products, aerosols, personal-care products, and detergents (NAEI, 2021). Solvent usage
 379 had become the largest contributory sector (33.7%) to VOCs emissions by 2019, followed by

380 industrial processes (16.0%).

381 As shown in Figure 4(a), the VOC speciation over the 1990-2019 period was dominated in mass
382 terms by contributions from alkanes and alcohols, the former decreasing as gasoline sources
383 declined, the other increasing as non-industrial solvent and food and drink industry processes
384 emissions followed a different pattern. Alkane emissions fell from 46.6% to 30.6% over the period.
385 Further reductions in alkane emissions are expected from policies for that phase-out sales of new
386 internal combustion engine vehicles in the UK (and in many other places) by 2035. Growth in the
387 relative contributions of alcohols was primarily driven by increases in emissions of methanol and
388 ethanol, and to a lesser extent in 1-butanol and 2-propanol (Figure 4(c)).



389
390 Figure 4. Contributions to annual national UK emissions of VOCs between 1990-2019 by: (a)
391 functional group; (b) by major emissions reporting sector; (c) for four individual alcohols in the
392 overall sub-class of alcohols; (d) for eight individual alkanes in the sub-class of all alkanes.

393

394 Figure S7 shows UK emission trends of individual species from different VOCs classes. These
395 highlight a national trend since 1990 of decreasing emissions of ethane associated with natural gas
396 leakage, toluene and propane associated with on-road petrol evaporation, as well as reductions of
397 benzene, ethene, and acetylene associated with tailpipe exhaust. Meanwhile, the reduced emissions
398 have been accompanied with increases in emissions of methanol and ethanol. The increase in
399 methanol is largely attributed to increased emissions from car-care products (i.e., non-aerosol

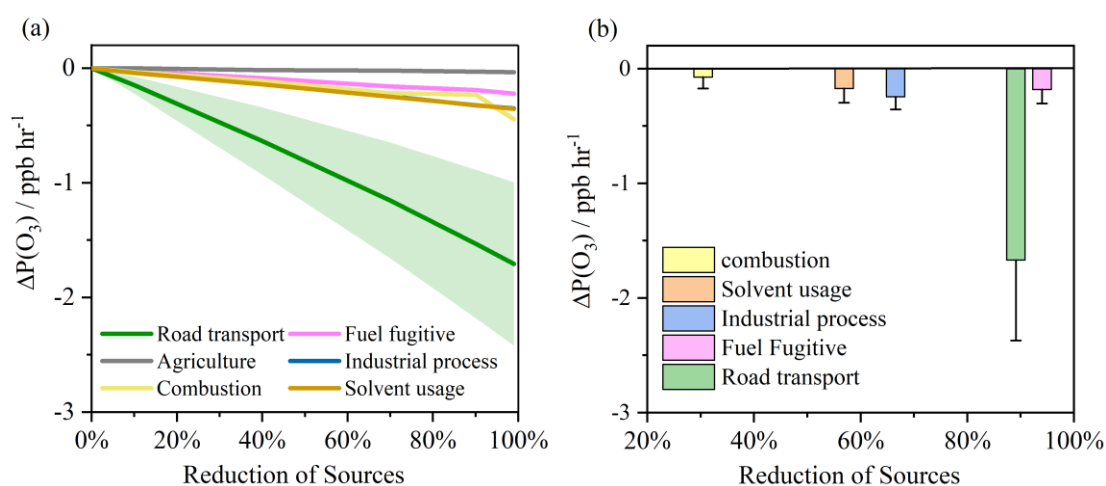
400 products). The increase in ethanol is due to increased domestic and industrial solvent usage.

401 The NO_x, CO, and VOC speciation within the NAEI for each of the six major emission sectors
402 was used to assign proportional sectoral contributions to the VOCs observed in Birmingham, and
403 hence to ozone production in the case study. (Table S5). **Isoprene was excluded from the analysis as
404 it is assumed to have an entirely biogenic source.** The six sectors are: road transport (both of on-
405 road exhaust emission and evaporative losses of fuel vapor), industrial processes, combustion,
406 solvent usage, fuel fugitive, and agriculture emissions). This makes a key assumption that the VOCs
407 at the observation site are affected directly in the same proportion that VOCs are reported in national
408 amounts in the NAEI. We make this assumption since it provides a reasonable starting point for
409 understanding how each VOC sector may influence O₃ production during a case study event,
410 however ozone formation might be sensitive to differing regional distribution in speciation. **The
411 attribution of VOCs sources based on the NAEI data can be thought of as representative for this
412 case study as a typical urban environment, but it might not hold for cities near large industrial VOC
413 sources (i.e., oil refinery and industrial production sites), since they can significantly affect
414 composition and chemical reactivity of ambient VOCs.**

415 Figure S8 shows the modelled RIRs for these sources in the initial, O₃, and clear-out periods.
416 All the sources generally showed higher RIR values in the O₃ period. Road transport exhibited the
417 highest positive RIR values in all periods (0.30 - 0.36), followed by industrial process (0.06 - 0.09)
418 and solvent usage (0.05 - 0.07). Despite being a relatively minor contributor to the mass of national
419 VOCs emissions (only 3.3% of the total in 2019), road transport VOCs still played the most
420 important role in local ozone photochemical chemistry, in this case study.

421 Figure 5a shows the changes in P(O₃) during the O₃ period from 08:00 to 16:00 which might
422 arise as a result of reductions in the individual sectors described above. **For this analysis, emission
423 changes in these sectors can be obtained by reducing model constrained concentrations of VOCs,
424 NO_x, and CO according to their contributions arising from individual emission sectors.** This is a
425 ‘thought experiment’ where under 2019 general observed atmospheric conditions (e.g., for NO_x, CO
426 and so on), each of the VOC source sectors is then further reduced in isolation (from 2019 levels)
427 and the effects on ΔP(O₃) were evaluated. Based on these scenarios, reducing emissions from the
428 individual sectors all resulted in decreased P(O₃), as would be anticipated. Reducing ozone
429 precursors arising from road transport would lead to a decreased P(O₃) of ~1.71 ppbv h⁻¹ if that

430 sector could be 100% abated in the case study. This is expected because road transport is a source
 431 of photochemically reactive VOCs, including aromatics, aldehyde, and short-chain alkanes/alkenes.
 432 Other sectors showed more modest effects, with reductions in solvent-related VOCs the next most
 433 significant lever to control ozone. Fully abating emissions of all industrial and solvent process
 434 emissions only resulted in a decreased $P(O_3)$ of ~ 0.35 ppbv h^{-1} , largely because they are dominated
 435 by ethanol and methanol with relatively low RIR values. Considering the real-world changes in
 436 VOC emissions over the period of 1990 to 2019, the very major reductions in road transport
 437 emissions have led to the largest effects in reducing $P(O_3)$ (Figure 5(b)). Whilst there have also been
 438 some very large reductions (94.6%) in fuel fugitive emissions, the impact on $P(O_3)$ reduction is
 439 modelled to have been relatively modest, being similar to industrial processes and solvent usage. **It**
 440 **is important to acknowledge the limitation of this analysis. In the real world, reductions in ambient**
 441 **VOCs from the NAEI sectors are affected by photochemical loss rate and advection processes,**
 442 **potentially altering the proportion of VOCs that would be observed with each sector reduction at**
 443 **the measurement site. This would potentially be an important consideration if instantaneously**
 444 **radical budgets were being evaluated, but it is a less significant issue when integrated ozone**
 445 **production effects.**

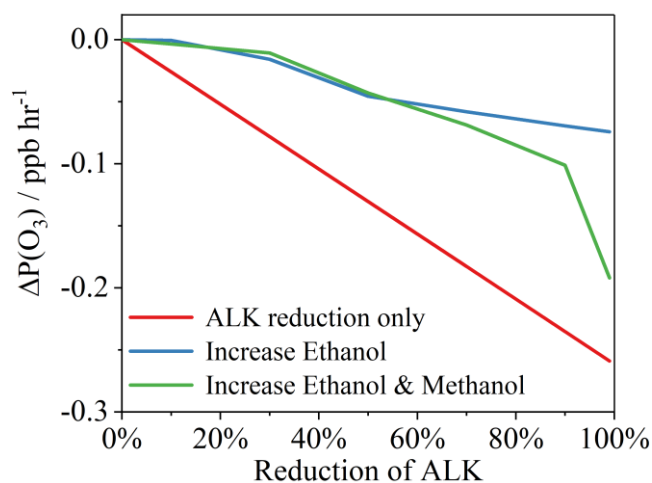


446
 447 Figure 5. (a) Changes in $P(O_3)$ in response to different reductions in VOCs, NO_x , and CO from
 448 different sectors for the Birmingham-case study condition. (b) Changes in $P(O_3)$ based on the NAEI
 449 estimated reductions in VOCs from different sectors between 1990 and 2019. The standard
 450 deviations represent variability in $\Delta P(O_3)$ during 08:00-16:00 LST in the O_3 period.

451

452 Further model runs were performed to better understand the impacts of the shift between

453 alkanes and alcohol species on $P(O_3)$, given trends showing decreasing alkanes emissions and
 454 increasing alcohol emissions between the 1990-2019 period (Figure 4). The modelled alkane
 455 concentrations in the case study were reduced by 10%, 30%, 50%, 70%, 90%, and 99%. This
 456 represents a downward trajectory in alkane emissions that would be anticipated as gasoline vehicles
 457 are slowly retired. Two further scenarios were then developed to sit alongside these reductions in
 458 alkanes. Firstly, the concentration of ethanol was increased to keep the overall total VOC
 459 concentrations in the model under case study conditions unchanged. Second, the concentration of
 460 both ethanol and methanol were scaled upwards to keep total VOCs concentration unchanged. As
 461 shown in Figure 6, reductions in alkanes alone resulted in decreased $P(O_3)$ to a maximum of ~ 0.26
 462 ppbv h^{-1} if fully abated. If that alkane reduction was balanced with increased ethanol and methanol,
 463 then $\Delta P(O_3)$ is reduced by a maximum of 0.19 ppbv h^{-1} . If alkane reductions were balanced by
 464 increasing ethanol alone, then $P(O_3)$ still decreases, but only up to 0.07 ppbv h^{-1} .



465
 466 Figure 6. Reductions in $\Delta P(O_3)$ based on reducing alkanes (ALK) in the model (under case study
 467 conditions), reducing alkanes but balancing the overall VOC amount with increased ethanol (blue
 468 line) and reducing alkanes but balancing the overall VOC amount with increased ethanol and
 469 methanol (green line).

470

471 Conclusion

472 In this study a typical high- O_3 event in Birmingham, United Kingdom was chosen as a case
 473 study to investigate the impacts of changes to VOCs emissions and speciation on urban O_3
 474 production. The *in-situ* O_3 formation sensitivity was split into three periods: initial, high O_3 , and

475 clear-out. Results from OH reactivity, O₃ budgets, and RIR index showed that O₃ formation in all
476 three periods was impacted by both VOCs and NO_x, but was more sensitive to anthropogenic VOCs.
477 The oxidation of alcohols and photolysis of acetaldehyde substantially contributed to *in-situ* O₃
478 formation, especially in the high O₃ period. The roles of anthropogenic VOC sources in urban O₃
479 chemistry were examined by integrating the NAEI speciation over the period of 1990-2019 into
480 photochemical box model scenarios. Despite road transport only contributing 3.3% of national
481 VOCs emissions in 2019 it still played the most important VOC role in the case study ozone
482 photochemistry, when inventory contributions were mapped onto observed VOCs. Sequentially the
483 observed VOCs were reduced by the fractional contributions and speciation in the NAEI for six
484 sectors to evaluate what impact abating different VOCs-emitting sectors would have on P(O₃).
485 Abating road transport VOCs in isolation would lead to a decreased P(O₃) by up to 1.67 ppbv h⁻¹,
486 but abating other sectors such as solvent use and fugitive fuels had noticeably smaller effects.
487 Despite emissions of VOCs from road transport falling very dramatically between 1990 and 2019,
488 it remains one of the most powerful means to further reduce ozone in this typical UK case study.
489 The wider shift in speciation reported in the NAEI from alkanes to alcohols was also examined
490 using scenarios where emission reductions for alkanes, were counterbalanced with increases in
491 alcohols, all simulated for the Birmingham case study conditions (e.g., for NO_x, CO and etc). Further
492 reducing alkanes from present day conditions to zero has a clear beneficial effect on reducing P(O₃)
493 by up to ~0.26 ppb hr⁻¹. However, this benefit would to a degree be offset should alcohol emissions
494 (for example from food and drink, and/or solvent use) increase to counterbalance those alkanes
495 reductions. Whilst simple alcohols are inherently less potent ozone-forming VOCs compared to the
496 mixture of VOCs from road transport, avoiding future growth in emissions remains important, since
497 they weaken the long-term benefits of road transport electrification and the phase out of internal
498 combustion engine vehicles.

499

500 **Data Availability**

501 Observational data including meteorological parameters and air pollutants used in this study are
502 available at https://github.com/nervouslee/Birmingham_CS.git. UK national emission inventory is
503 available at <https://naei.beis.gov.uk/>.

504

505 **Author Contribution**

506 Jianghao Li prepared the manuscript with contributions from all authors. Alastair C. Lewis helped
507 with modelling scenarios and revised the manuscript. Jim R. Hopkins contributed to measurement
508 of chemical species. Stephen J. Andrews contributed to scientific discussion on findings of this work.
509 Tim Murrells, Neil Passant and Ben Richmond contributed to the data of national emission inventory
510 data and revision on NAEI methodology. Siqu Hou, William J. Bloss, Roy M. Harrison, and Zongbo
511 Shi provided measurements of atmospheric pollutants used in this study, along with critical
512 discussion on revising the manuscript.

513

514 **Competing interests**

515 The authors declare that they have no conflict of interest.

516

517 **Acknowledgements**

518 Establishment and operation of the Birmingham Air Quality Supersite operation (BAQS) is
519 supported by the NERC WM-Air project (NE/S003487/1) and UKRI Clean Air SPF project OSCA
520 (NE/T001976/1). This work forms part of the National Centre for Atmospheric Science National
521 Capability programme funded by NERC. Jianghao Li's study at the University of York is financially
522 supported by the China Scholarship Council (grant no. 202206560052).

523

524 **References**

525 Abernethy, S., O'Connor, F., Jones, C., and Jackson, R.: Methane removal and the proportional
526 reductions in surface temperature and ozone, *Philosophical Transactions of the Royal Society*
527 *A*, 379, 20210104, 10.1098/rsta.2021.0104, 2021.

528 Calvert, J. G., Orlando, J. J., Stockwell, W. R., and Wallington, T. J.: *The mechanisms of reactions*
529 *influencing atmospheric ozone*, Oxford University Press, USA, 2015.

530 Chen, T., Xue, L., Zheng, P., Zhang, Y., Liu, Y., Sun, J., Han, G., Li, H., Zhang, X., and Li, Y.:
531 Volatile organic compounds and ozone air pollution in an oil production region in northern
532 China, *Atmospheric Chemistry and Physics*, 20, 7069-7086, 10.5194/acp-20-7069-2020, 2020.

533 Cliff, S. J., Lewis, A. C., Shaw, M. D., Lee, J. D., Flynn, M., Andrews, S. J., Hopkins, J. R., Purvis,

534 R. M., and Yeoman, A. M.: Unreported VOC emissions from road transport including from
535 electric vehicles, *Environmental Science & Technology*, 10.1021/acs.est.3c00845, 2023.

536 Coggon, M. M., Gkatzelis, G. I., McDonald, B. C., Gilman, J. B., Schwantes, R. H., Abuhassan, N.,
537 Aikin, K. C., Arend, M. F., Berkoff, T. A., Brown, S. S., Campos, T. L., Dickerson, R. R.,
538 Gronoff, G., Hurley, J. F., Isaacman-VanWertz, G., Koss, A. R., Li, M., McKeen, S. A.,
539 Moshary, F., Peischl, J., Pospisilova, V., Ren, X., Wilson, A., Wu, Y., Trainer, M., and Warneke,
540 C.: Volatile chemical product emissions enhance ozone and modulate urban chemistry, *Proc
541 Natl Acad Sci U S A*, 118, 10.1073/pnas.2026653118, 2021.

542 de Foy, B., Brune, W. H., and Schauer, J. J.: Changes in ozone photochemical regime in Fresno,
543 California from 1994 to 2018 deduced from changes in the weekend effect, *Environmental
544 Pollution*, 263, 114380, 10.1016/j.envpol.2020.114380, 2020.

545 Department for Environment, Food & Rural Affairs. An annual update of data on concentrations of
546 major air pollutants in the UK: [https://www.gov.uk/government/statistical-data-sets/env02-air-
547 quality-statistics](https://www.gov.uk/government/statistical-data-sets/env02-air-quality-statistics), last access: 07 September 2023.

548 Diaz, F. M., Khan, M. A. H., Shallcross, B. M., Shallcross, E. D., Vogt, U., and Shallcross, D. E.:
549 Ozone trends in the United Kingdom over the last 30 years, *Atmosphere*, 11, 534,
550 10.3390/atmos11050534, 2020.

551 Edwards, P. M., Brown, S. S., Roberts, J. M., Ahmadov, R., Banta, R. M., deGouw, J. A., Dube, W.
552 P., Field, R. A., Flynn, J. H., Gilman, J. B., Graus, M., Helmig, D., Koss, A., Langford, A. O.,
553 Lefer, B. L., Lerner, B. M., Li, R., Li, S. M., McKeen, S. A., Murphy, S. M., Parrish, D. D.,
554 Senff, C. J., Soltis, J., Stutz, J., Sweeney, C., Thompson, C. R., Trainer, M. K., Tsai, C., Veres,
555 P. R., Washenfelder, R. A., Warneke, C., Wild, R. J., Young, C. J., Yuan, B., and Zamora, R.:
556 High winter ozone pollution from carbonyl photolysis in an oil and gas basin, *Nature*, 514,
557 351-354, 10.1038/nature13767, 2014.

558 European Environment Agency.: EMEP/EEA air pollutant emission inventory guidebook 2016,
559 2016. <https://www.eea.europa.eu/publications/emep-eea-guidebook-2016>, last access 07
560 September 2023.

561 Finch, D. P. and Palmer, P. I.: Increasing ambient surface ozone levels over the UK accompanied by
562 fewer extreme events, *Atmospheric environment*, 237, 117627,
563 10.1016/j.atmosenv.2020.117627, 2020.

564 Gaudel, A., Cooper, O. R., Chang, K.-L., Bourgeois, I., Ziemke, J. R., Strode, S. A., Oman, L. D.,
565 Sellitto, P., Nédélec, P., Blot, R., Thouret, V., and Granier, C.: Aircraft observations since the
566 1990s reveal increases of tropospheric ozone at multiple locations across the Northern
567 Hemisphere, *Science Advances*, 6, eaba8272, doi:10.1126/sciadv.aba8272, 2020.

568 Gkatzelis, G. I., Coggon, M. M., McDonald, B. C., Peischl, J., Aikin, K. C., Gilman, J. B., Trainer,
569 M., and Warneke, C.: Identifying volatile chemical product tracer compounds in US cities,
570 *Environmental Science & Technology*, 55, 188-199, 10.1021/acs.est.0c05467, 2021.

571 Gouldsbrough, L., Hossaini, R., Eastoe, E., and Young, P. J.: A temperature dependent extreme value
572 analysis of UK surface ozone, 1980–2019, *Atmospheric Environment*, 273, 118975,

573 [10.1016/j.atmosenv.2022.118975](https://doi.org/10.1016/j.atmosenv.2022.118975), 2022.

574 Gouldsbrough, L., Hossaini, R., Eastoe, E., Young, P. J., and Vieno, M.: A machine learning
575 approach to downscale EMEP4UK: analysis of UK ozone variability and trends, *Atmospheric*
576 *Chemistry and Physics*, 24, 3163-3196, [10.5194/acp-24-3163-2024](https://doi.org/10.5194/acp-24-3163-2024), 2024.

577 He, Z., Wang, X., Ling, Z., Zhao, J., Guo, H., Shao, M., and Wang, Z.: Contributions of different
578 anthropogenic volatile organic compound sources to ozone formation at a receptor site in the
579 Pearl River Delta region and its policy implications, *Atmospheric Chemistry and Physics*, 19,
580 8801-8816, [10.5194/acp-19-8801-2019](https://doi.org/10.5194/acp-19-8801-2019), 2019.

581 Hertig, E., Russo, A., and Trigo, R. M.: Heat and ozone pollution waves in central and south
582 Europe—characteristics, weather types, and association with mortality, *Atmosphere*, 11, 1271,
583 [10.3390/atmos11121271](https://doi.org/10.3390/atmos11121271), 2020.

584 Ivatt, P. D., Evans, M. J., and Lewis, A. C.: Suppression of surface ozone by an aerosol-inhibited
585 photochemical ozone regime, *Nature Geoscience*, 15, 536-540, [10.1038/s41561-022-00972-9](https://doi.org/10.1038/s41561-022-00972-9),
586 2022.

587 Jenkin, M., Saunders, S., Wagner, V., and Pilling, M.: Protocol for the development of the Master
588 Chemical Mechanism, MCM v3 (Part B): tropospheric degradation of aromatic volatile organic
589 compounds, *Atmospheric Chemistry and Physics*, 3, 181-193, [10.5194/acp-3-181-2003](https://doi.org/10.5194/acp-3-181-2003), 2003.

590 Kang, M., Hu, J., Zhang, H., and Ying, Q.: Evaluation of a highly condensed SAPRC chemical
591 mechanism and two emission inventories for ozone source apportionment and emission control
592 strategy assessments in China, *Science of The Total Environment*, 813, 151922,
593 [10.1016/j.scitotenv.2021.151922](https://doi.org/10.1016/j.scitotenv.2021.151922), 2022.

594 Kumar, P., Kuttippurath, J., von der Gathen, P., Petropavlovskikh, I., Johnson, B., McClure-Begley,
595 A., Cristofanelli, P., Bonasoni, P., Barlasina, M. E., and Sanchez, R.: The Increasing Surface
596 Ozone and Tropospheric Ozone in Antarctica and Their Possible Drivers, *Environmental*
597 *Science & Technology*, 55, 8542-8553, [10.1021/acs.est.0c08491](https://doi.org/10.1021/acs.est.0c08491), 2021.

598 Lee, J. D., Drysdale, W. S., Finch, D. P., Wilde, S. E., and Palmer, P. I.: UK surface NO₂ levels
599 dropped by 42% during the COVID-19 lockdown: impact on surface O₃, *Atmospheric*
600 *Chemistry and Physics*, 20, 15743-15759, [10.5194/acp-20-15743-2020](https://doi.org/10.5194/acp-20-15743-2020), 2020.

601 Lefohn, A. S., Malley, C. S., Smith, L., Wells, B., Hazucha, M., Simon, H., Naik, V., Mills, G.,
602 Schultz, M. G., Paoletti, E., De Marco, A., Xu, X., Zhang, L., Wang, T., Neufeld, H. S.,
603 Musselman, R. C., Tarasick, D., Brauer, M., Feng, Z., Tang, H., Kobayashi, K., Sicard, P.,
604 Solberg, S., and Gerosa, G.: Tropospheric ozone assessment report: Global ozone metrics for
605 climate change, human health, and crop/ecosystem research, *Elementa: Science of the*
606 *Anthropocene*, 6, [10.1525/elementa.279](https://doi.org/10.1525/elementa.279), 2018.

607 Lewis, A. C., Allan, J. D., Carruthers, D., Carslaw, D. C., Fuller, G. W., Harrison, R. M., Heal, M.
608 R., Nemitz, E., Reeves, C., Williams, M., Fowler, D., Marnier, B. B., Williams, A., Carslaw, N.,
609 Moller, S., Maggs, R., Murrells, T., Quincey, P., and Willis, P.: Ozone in the UK: Recent Trends
610 and Future Projections. Air Quality Expert Group. [https://uk-](https://uk-air.defra.gov.uk/library/reports.php?report_id=1064)
611 [air.defra.gov.uk/library/reports.php?report_id=1064](https://uk-air.defra.gov.uk/library/reports.php?report_id=1064), 2021, last assess: 27 March 2024.

612 Lewis, A. C., Hopkins, J. R., Carslaw, D. C., Hamilton, J. F., Nelson, B. S., Stewart, G., Dornie, J.,
613 Passant, N., and Murrells, T.: An increasing role for solvent emissions and implications for
614 future measurements of volatile organic compounds, *Philosophical Transactions of the Royal*
615 *Society A*, 378, 20190328, 10.1098/rsta.2019.0328, 2020.

616 Li, J., Yu, Z., Du, Z., Ji, Y., and Liu, C.: Standoff chemical detection using laser absorption
617 spectroscopy: a review, *Remote Sensing*, 12, 2771, 10.3390/rs12172771, 2020.

618 Liu, Q., Gao, Y., Huang, W., Ling, Z., Wang, Z., and Wang, X.: Carbonyl compounds in the
619 atmosphere: A review of abundance, source and their contributions to O₃ and SOA formation,
620 *Atmospheric Research*, 106184, 10.1016/j.atmosres.2022.106184, 2022a.

621 Liu, T., Hong, Y., Li, M., Xu, L., Chen, J., Bian, Y., Yang, C., Dan, Y., Zhang, Y., and Xue, L.:
622 Atmospheric oxidation capacity and ozone pollution mechanism in a coastal city of
623 southeastern China: analysis of a typical photochemical episode by an observation-based
624 model, *Atmospheric Chemistry and Physics*, 22, 2173-2190, 10.5194/acp-22-2173-2022,
625 2022b.

626 Liu, Z., Doherty, R. M., Wild, O., O'connor, F. M., and Turnock, S. T.: Tropospheric ozone changes
627 and ozone sensitivity from the present day to the future under shared socio-economic pathways,
628 *Atmospheric Chemistry and Physics*, 22, 1209-1227, 10.5194/acp-22-1209-2022, 2022.

629 McDonald, B. C., De Gouw, J. A., Gilman, J. B., Jathar, S. H., Akherati, A., Cappa, C. D., Jimenez,
630 J. L., Lee-Taylor, J., Hayes, P. L., and McKeen, S. A.: Volatile chemical products emerging as
631 largest petrochemical source of urban organic emissions, *Science*, 359, 760-764,
632 10.1126/science.aaq0524, 2018.

633 Monks, P. S., Allan, J. D., Carruthers, D., Carslaw, D. C., Fuller, G. W., Harrison, R. M., Heal, M.
634 R., Lewis, A. C., Nemitz, E., Reeves, C., Williams, M., Fowler, D., Marnner, B. B., Williams,
635 A., Moller, S., Maggs, R., Murrells, T., Quincey, P., and Willis, P.: Non-methane Volatile
636 Organic Compounds in the UK, Air Quality Group. [https://uk-](https://uk-air.defra.gov.uk/library/reports.php?report_id=10032020)
637 [air.defra.gov.uk/library/reports.php?report_id=10032020](https://uk-air.defra.gov.uk/library/reports.php?report_id=10032020), 2020, last access: 07 September
638 2023.

639 National Atmospheric Emissions Inventory.: UK Informative Inventory Report (1990 to 2019),
640 2021. https://naei.beis.gov.uk/reports/reports?report_id=1016, last access: 07 September 2023.

641 Nelson, B. S., Stewart, G. J., Drysdale, W. S., Newland, M. J., Vaughan, A. R., Dunmore, R. E.,
642 Edwards, P. M., Lewis, A. C., Hamilton, J. F., and Acton, W. J.: In situ ozone production is
643 highly sensitive to volatile organic compounds in Delhi, India, *Atmospheric Chemistry and*
644 *Physics*, 21, 13609-13630, 10.5194/acp-21-13609-2021, 2021.

645 Qin, M., Murphy, B. N., Isaacs, K. K., McDonald, B. C., Lu, Q., McKeen, S. A., Koval, L., Robinson,
646 A. L., Efstathiou, C., and Allen, C.: Criteria pollutant impacts of volatile chemical products
647 informed by near-field modelling, *Nature sustainability*, 4, 129-137, 10.1038/s41893-020-
648 00614-1, 2021.

649 Saunders, S. M., Jenkin, M. E., Derwent, R., and Pilling, M.: Protocol for the development of the
650 Master Chemical Mechanism, MCM v3 (Part A): tropospheric degradation of non-aromatic

651 volatile organic compounds, *Atmospheric Chemistry and Physics*, 3, 161-180, 10.5194/acp-3-
652 161-2003, 2003.

653 Schroeder, J. R., Crawford, J. H., Ahn, J.-Y., Chang, L., Fried, A., Walega, J., Weinheimer, A.,
654 Montzka, D. D., Hall, S. R., and Ullmann, K.: Observation-based modeling of ozone chemistry
655 in the Seoul metropolitan area during the Korea-United States Air Quality Study (KORUS-
656 AQ), *Elementa: Science of the Anthropocene*, 8, 3, 10.1525/elementa.400, 2020.

657 Seinfeld, J. H. and Pandis, S. N.: *Atmospheric chemistry and physics: from air pollution to climate*
658 *change*, John Wiley & Sons, 2016.

659 Sicard, P.: Ground-level ozone over time: an observation-based global overview, *Current Opinion*
660 *in Environmental Science & Health*, 19, 100226, 10.1016/j.eti.2022.102809, 2021.

661 Sicard, P., Paoletti, E., Agathokleous, E., Araminienè, V., Proietti, C., Coulibaly, F., and De Marco,
662 A.: Ozone weekend effect in cities: Deep insights for urban air pollution control,
663 *Environmental Research*, 191, 110193, 10.1016/j.envres.2020.110193, 2020.

664 Tarasick, D., Galbally, I. E., Cooper, O. R., Schultz, M. G., Ancellet, G., Leblanc, T., Wallington, T.
665 J., Ziemke, J., Liu, X., and Steinbacher, M.: Tropospheric Ozone Assessment Report:
666 Tropospheric ozone from 1877 to 2016, observed levels, trends and uncertainties, *Elementa:*
667 *Science of the Anthropocene*, 7, 39, 10.1525/elementa.376, 2019.

668 Wang, S., Yuan, B., Wu, C., Wang, C., Li, T., He, X., Huangfu, Y., Qi, J., Li, X.-B., and Sha, Q. e.:
669 Oxygenated volatile organic compounds (VOCs) as significant but varied contributors to VOC
670 emissions from vehicles, *Atmospheric Chemistry and Physics*, 22, 9703-9720, 10.5194/acp-
671 22-9703-2022, 2022.

672 Wang, Y., Guo, H., Zou, S., Lyu, X., Ling, Z., Cheng, H., and Zeren, Y.: Surface O₃ photochemistry
673 over the South China Sea: Application of a near-explicit chemical mechanism box model,
674 *Environmental Pollution*, 234, 155-166, 10.1016/j.envpol.2017.11.001, 2018.

675 Warburton, T., Grange, S. K., Hopkins, J. R., Andrews, S. J., Lewis, A. C., Owen, N., Jordan, C.,
676 Adamson, G., and Xia, B.: The impact of plug-in fragrance diffusers on residential indoor VOC
677 concentrations, *Environmental Science: Processes & Impacts*, 25, 805-817,
678 10.1039/D2EM00444E, 2023.

679 Winkler, S., Anderson, J., Garza, L., Ruona, W., Vogt, R., and Wallington, T.: Vehicle criteria
680 pollutant (PM, NO_x, CO, HCs) emissions: how low should we go?, *Npj Climate and*
681 *atmospheric science*, 1, 26, 10.1038/s41612-018-0037-5, 2018.

682 Wolfe, G. M., Marvin, M. R., Roberts, S. J., Travis, K. R., and Liao, J.: The framework for 0-D
683 atmospheric modeling (F0AM) v3. 1, *Geoscientific Model Development*, 9, 3309-3319,
684 10.5194/gmd-9-3309-2016, 2016.

685 Wu, R. and Xie, S.: Spatial Distribution of Ozone Formation in China Derived from Emissions of
686 Speciated Volatile Organic Compounds, *Environmental Science & Technology*, 51, 2574-2583,
687 10.1021/acs.est.6b03634, 2017.

688 Yeoman, A. M. and Lewis, A. C.: Global emissions of VOCs from compressed aerosol products,
689 *Elementa: Science of the Anthropocene*, 9, 00177, 10.1525/elementa.2020.20.00177, 2021.

690 Zulkifli, M. F. H., Hawari, N. S. S. L., Latif, M. T., Abd Hamid, H. H., Mohtar, A. A. A., Idris, W.
691 M. R. W., Mustaffa, N. I. H., and Juneng, L.: Volatile organic compounds and their contribution
692 to ground-level ozone formation in a tropical urban environment, *Chemosphere*, 302, 134852,
693 10.1016/j.chemosphere.2022.134852, 2022.
694